Study on the lipid organization of stratum corneum lipid models by (cryo-) electron diffraction

G. S. K. Pilgram,[1,*] A. M. Engelsma-van Pelt,[*] G. T. Oostergetel,[†] H. K. Koerten,[*] J. A. Bouwstra[§]

Laboratory for Electron Microscopy,* Leiden University Medical Center, P.O. Box 9503, 2300 RA Leiden, The Netherlands; Groningen Biomolecular Sciences and Biotechnology Institute,† University of Groningen, Nijenborgh 4, 9747 AG Groningen, The Netherlands; and Leiden/Amsterdam Center for Drug Research,§ Leiden University, P.O. Box 9502, 2300 RA Leiden, The Netherlands

Abstract **The barrier function of the skin resides in the stratum corneum (SC). This outermost layer consists of protein-rich corneocytes and lipid-rich intercellular domains. These domains form the rate-limiting step for transepidermal water loss and the penetration of substances from the environment. To study the nature of the barrier function, stratum corneum lipid models have been examined with wide-angle X-ray diffraction. A disadvantage of this technique is that it requires bulk quantities of lipid and thus information on variations in the lateral packing cannot be obtained in the μm-range. To the best of our knowledge, this is the first study in which electron diffraction is applied on SC lipid model systems. Using this technique, local structural information was obtained about mixtures prepared from isolated pig ceramides, cholesterol, and long-chain free fatty acids. It appeared that addition of free fatty acids caused a transition from a hexagonal to an orthorhombic packing and that electron diffraction can be applied to distinguish between these two lattices. The results are in good agreement with wide-angle X-ray diffraction data and suggest that application of electron diffraction in skin studies can provide new information on the lipid organization in well-defined areas of the stratum corneum.—**Pilgram, G. S. K., A. M. Engelsma-van Pelt, G. T. Oostergetel, H. K. Koerten, and J. A. Bouwstra. **Study on the lipid organization of stratum corneum lipid models by (cryo-)electron diffraction.** ***J. Lipid. Res.*** 39: **1669–1676.**

Supplementary key words skin • ceramides • lipids • WAXD • barrier function • hexagonal • orthorhombic • lateral packing • biological crystals

The stratum corneum (SC) forms a relatively impermeable layer at the surface of mammalian skin to hinder the evaporation of water and the penetration of agents across the skin (1). This barrier function is the result of the unique structure and composition of the SC. The SC consists of two compartments: the flat, keratinized corneocytes and the lipid-rich intercellular domains (2). This latter compartment forms a continuous phase surrounding the corneocytes. Thus, percutaneous absorption of substances will always involve the intercellular domains (3, 4), which therefore play a key role in the barrier function of the skin (5). In order to get insight in the nature of this barrier function, the lipid organization has been examined in SC lipid models of various compositions and at variable hydration state, pH, and temperature (6–11). The aim of our study is to obtain detailed information about the lateral lipid organization in a model system resembling the lipid composition of the SC using (cryo-) electron diffraction (ED).

The basic chemical composition of the SC differs significantly from viable tissues, which indicates the uniqueness of the SC. Especially, its low water content (15% in vivo) is a striking feature (12). Most of this water is present in the corneocytes, while the intercellular lamellae have a low hydration state (13). Increased hydration causes swelling of the corneocytes, while swelling of the lipid lamellae or a change in the lateral packing has not been observed (14–16). However, increasing the hydration of the SC above 30–40% results in a diminution of the skin barrier function (17) and in an increase of the chain mobility of the acyl chains, as observed using electron spin resonance (18).

The intercellular domains primarily contain ceramides (type 1 to 6), cholesterol, and free fatty acids and to a lesser extent cholesterol sulfate (19). These molecules are arranged in stacked bilayers that have been visualized in freeze fracture studies (5, 20) and by ruthenium tetroxide staining of transverse SC sections (21, 22). Small-angle X-ray diffraction (SAXD) studies on human and pig SC showed that these bilayers form two lamellar phases with periodicities of approximately 13 and 6 nm (23, 24). To study the lateral lipid organization of the intercellular domains, techniques such as atomic force microscopy (25), Fourier transformed infrared spectroscopy (26) and wide-

Abbreviations: ED, electron diffraction; WAXD, wide-angle X-ray diffraction; SAXD, small-angle X-ray diffraction; SC, stratum corneum; CER, pure total ceramides isolated from pig skin; CHOL, cholesterol; FFA, free fatty acids; RT, room temperature; TEM, transmission electron microscope.

[1] To whom correspondence should be addressed.

Downloaded from www.jlr.org by guest, on June 14, 2012

angle X-ray diffraction (WAXD) have been used. The WAXD studies revealed that the lipids in human, pig, and murine SC can be arranged in either a liquid, a gel (hexagonal), or a crystalline (orthorhombic) packing with periodicities of approximately 0.46, 0.412, and 0.415/0.375 nm, respectively (24, 27, 28).

However, WAXD provides structural information on bulk quantities of SC, so that local variations in the lateral packing of the SC cannot be determined. Furthermore, these samples give rise to ring patterns, because the unit cells are present in a large range of orientations. This makes discrimination between the hexagonal (0.41 nm) and orthorhombic (0.41 and 0.37 nm) packing of the lipids and their orientation difficult on the basis of the characteristic reflections (15, 28). Thus, when both reflections are present in the X-ray diffraction pattern, higher order reflections characteristic for the hexagonal lattice are needed, to determine whether or not this packing is also present. However, these reflections are faint compared to the 0.41 and 0.37 nm reflections and differ only in the pm-range from higher order orthorhombic reflections. Therefore, it will be advantageous to be able to distinguish between the hexagonal and orthorhombic lattices on the basis of the 0.41 and 0.37 nm reflections.

In previous studies, we showed that ED can be applied as a tool to study the lateral lipid packing locally in human SC (29, 30). We hypothesize, therefore, that this technique has the potential to elucidate the lateral lipid organization in SC in more detail.

In the present study, we prepared lipid models from isolated ceramides of pig skin, cholesterol, and long-chain free fatty acids. From WAXD studies it is known that free fatty acids have an influence on the transition from a hexagonal to an orthorhombic packing of SC lipids (11). Therefore, the hexagonal and orthorhombic lattices could be studied in relation to the presence of free fatty acids in the lipid mixture. Furthermore, we compared the results of ED with WAXD data in order to explore whether ED can be applied to draw a more precise distinction between the hexagonal and orthorhombic lattices at the μm scale.

MATERIAL AND METHODS

Stratum corneum lipid models

We prepared dry lipid mixtures with different molar ratios of ceramides type 1 to 6 (CER) isolated from pig skin, cholesterol (CHOL), and/or long-chain (C26:0, C24:0, C22:0, C18:0, C16:0 in a molar ratio of 6.7:36.8:41.7:3.2:1.3) free fatty acids (FFA). The method for the isolation of the ceramides has been reported elsewhere (8). As controls, samples containing only ceramides or cholesterol were prepared. The lipids in each mixture were dissolved in chloroform–methanol 2:1 (v/v) with a final concentration of 8 μg/μl. A Camag Linomat IV was used to nebulize about 25 μg of each of the following mixtures (in molar ratios) onto a plain 400-mesh copper grid: *1*) pure CER, *2*) pure CHOL, *3*) CER/CHOL = 1:1, *4*) CER/CHOL = 2:1, *5*) CER/CHOL/FFA = 1:1:1. The samples were stored under gaseous nitrogen at room temperature (RT) or at −20°C and equilibrated at RT during 24 h, before examination in the transmission electron microscope (TEM). The temperatures in this procedure are all below the transition temperatures of the lipids and should, therefore, not influence their organization.

Visualization and electron diffraction

The diffraction patterns of the different lipid samples were recorded at RT and at −170°C. Therefore, grids containing the lipid mixtures were either placed in a conventional specimen-holder or in a cryo-holder (Gatan Cryo Transfer System, Model 626) at RT and inserted into a Philips EM400T or a Philips CM200FEG transmission electron microscope. The cryo-holder was cooled to −170°C by liquid nitrogen after an equilibration time of 30 min in order to avoid the formation of ice-crystals during the cooling procedure. The EM400T operated at 100 kV, which corresponds to a wavelength of 0.0037 nm, and the CM200FEG at 200 kV (λ = 0.0025 nm). ED patterns from areas with a diameter of 1 μm (about 1 μm^2) or 5 μm (about 20 μm^2) were recorded on Kodak Electron Microscope films 4489 (EM400T) or using a cooled slow-scan CCD camera (Gatan type 794) (CM200FEG) with a low beam intensity (dose rate approximately 10 $e^-/nm^2 \cdot s$) at a camera length of 290 or 360 mm, respectively. The exposure times varied between 2 and 10 seconds, yielding an electron dose on the specimen of approximately 50 e^-/nm^2.

At least three samples of each mixture were examined and 5 to 20 diffraction patterns of each sample were recorded. The spacings of the reflections in the diffraction patterns were calculated using the formula Rd = λL, which is deduced from the Bragg law (R = radius that is the distance from a reflection to central spot, d = spacing of the lattice plane, λ = wave length of the incident electron beam, L = camera length). The diffraction pattern of gold was used to calibrate the constant factor λL. Of each sample, the diameters (2R) of the reflections on 5 different recordings were measured (vernier caliper gauge) in three different directions to determine the spacing. An independent-samples T test was used to establish significant differences between the mean spacings calculated from each set of ED patterns as obtained from the different lipid models at RT and −170°C.

RESULTS

In this study, we prepared dry lipid samples by spraying various lipid mixtures onto plain 400-mesh copper grids in order to investigate these samples in the diffraction mode of the TEM. Support films, e.g., of formvar or pioloform, were not used to reduce diffuse scattering, which may make distinction of the ED patterns of lipids more difficult. We could establish that the lipid films of each sample were sufficiently self-supporting on the grids and were so stable that charging and tearing of the films hardly occurred during ED. Various electron densities could be observed in the samples (**Fig. 1**). These different electron densities were interpreted as variations in the thickness of the sample, caused by the variable number of lipid layers. Electron lucent areas were most suited for electron diffraction.

Electron diffraction

The diffraction patterns of the lipids were obtained from areas with a diameter of 5 or 1 μm and depending on the sizes of the selected areas, diffraction patterns could be recorded that consisted of rings or arcs (streaks), respectively. However, areas without clear ED patterns or

Downloaded from www.jlr.org by guest, on June 14, 2012

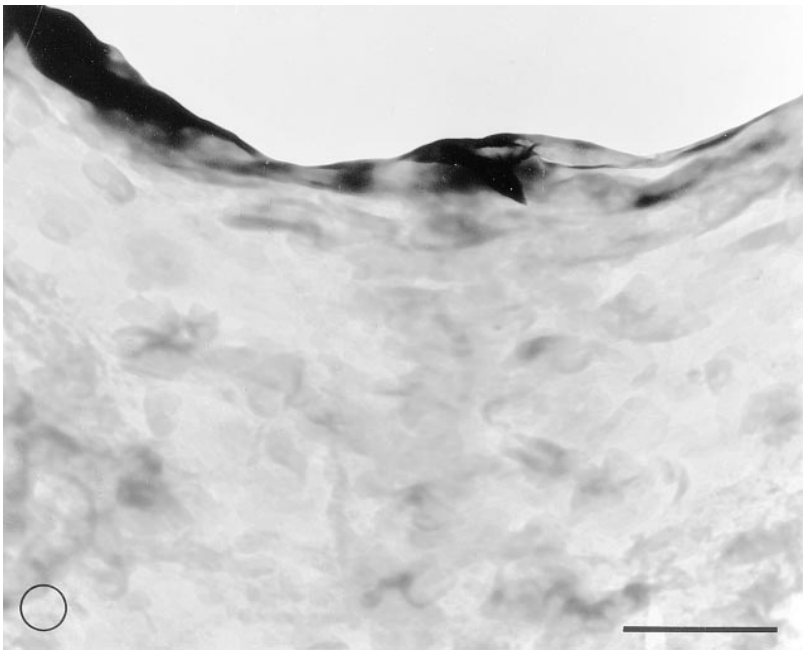

Fig. 1. Transmission electron micrograph of a lipid film formed by nebulizing the CER/CHOL/FFA mixture onto a grid. The differences in transparency are due to variations in the number of stacked lipid layers. The electron lucent areas are most suited for diffraction. Note the circle that indicates an area of 1 μm^2 that can be selected for diffraction. The beam diameter to select an area of 20 μm^2 is indicated by the scale bar (scale bar is 5 μm).

with only two opposite arcs were present as well. The spacings that were measured were mostly derived from the 0.41 nm and 0.37 nm lattice planes. Occasionally, more faint reflections from other lattice planes were recorded. Besides calculation of the lattice spacings, additional information could be obtained from the diffraction patterns with arc-shaped reflections by measuring the angles between the reciprocal lattice vectors and the angular width of the arcs. This width (expressed in degrees) gives an indication of misalignment or of the range of orientations of the unit cells.

The resulting spacings of the lipid models recorded at RT and at −170°C are given in **Table 1**. The spacings measured at both temperatures do not differ significantly, while radiation damage was reduced under cryo-conditions. This resulted in an improved stability of the sample, which allowed at least a 2-fold increase of the recording time. For convenience of the description of the ED results below, reference will be made to spacings measured at −170°C.

The diffraction patterns of the CHOL samples consisted of many reflections ranging from 0.70 to 0.48 nm that appeared as spots, regardless of the size of the area from which the diffraction pattern was obtained. The most frequently observed spacings were 0.68, 0.56, 0.52, 0.51, and 0.48 nm (**Fig. 2a**). The diffraction patterns of CER samples displayed a ring at 0.400 ± 0.005 nm when the area selected for diffraction had a diameter of 5 μm. However, when a smaller area of higher transparency was selected, a diffraction pattern could be recorded consisting of 6 opposite arcs at the same spacing. Occasionally, separate spots could be recognized within the arcs (Fig. 2b). The angles between the reciprocal lattice vectors were 60° ± 2° and the arcs subtended an angle of approximately 25°.

The CER/CHOL 1:1 samples showed diffraction patterns that consisted of spots at small diffraction angles, corresponding to 0.58, 0.52, 0.51, and 0.48 nm and a ring (**Fig. 3a**) or arcs at a spacing of 0.412 ± 0.004 nm depending on the size of the irradiated area. The diffraction pattern of the CER/CHOL 2:1 mixture also consisted of a ring at a spacing of 0.412 ± 0.001 nm. Spots at smaller diffraction angles were generally not observed in the ED patterns of this CER/CHOL mixture. The 0.412 nm reflections could appear as 3 pairs of opposite arcs when the beam diameter was decreased to 1 μm (Fig. 3b). The angles between the reciprocal lattice vectors of both CER/CHOL mixtures were 60° ± 1° and the angular width of the arcs was approximately 15°.

TABLE 1. List of the spacings measured from the electron diffraction patterns of the different lipid mixtures

	Ceramide	CER/CHOL 1:1	CER/CHOL 2:1	CER/CHOL/FFA 1:1:1
Room temperature	0.399 ± 0.007	0.412 ± 0.001	0.413 ± 0.003	0.413 ± 0.003/ 0.374 ± 0.007
−170°C	0.400 ± 0.005	0.412 ± 0.004	0.412 ± 0.001	0.414 ± 0.001/ 0.367 ± 0.001
Attribute to	hexagonal	hexagonal	hexagonal	orthorhombic

Upon addition of FFA to the SC lipid model system, a transition occurs from the non-crystalline hexagonal lipid packing to the crystalline orthorhombic packing.

Downloaded from www.jlr.org by guest, on June 14, 2012

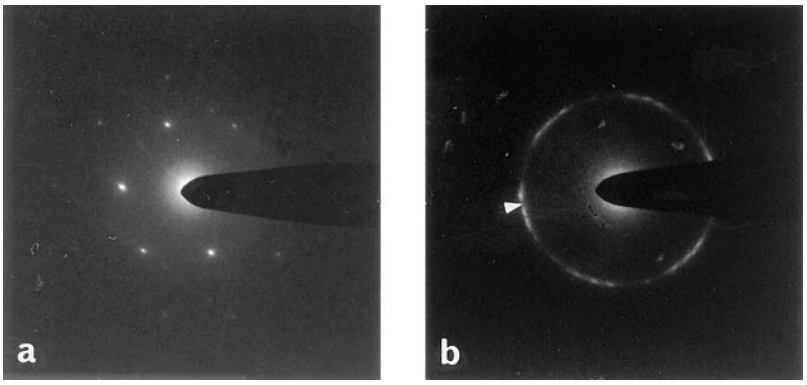

Fig. 2. Electron diffraction patterns of a: pure CHOL sample with spacings of 0.56 and 0.48 nm and b: pure CER sample with a spacing of 0.40 nm. The angles between the reciprocal lattice vectors are 60° and the angular width is approximately 20°. The arrowhead indicates the reflection with a stronger intensity.

The CER/CHOL/FFA mixture produced a different diffraction pattern. Two rings with spacings at 0.414 ± 0.001 nm and 0.367 ± 0.001 nm were recorded in the diffraction pattern obtained from an area of 20 μm^2 and occasionally two faint rings at 0.25 and 0.22 nm were also detected (**Fig. 4a**). Sometimes, spots at spacings between 0.70 and 0.48 nm, corresponding to those observed in the CHOL and CER/CHOL 1:1 samples, were present. When an area of 1 μm^2 was selected for diffraction, ED patterns could be recorded that consisted of two pairs of opposite arcs at 0.414 nm and a more faint pair of arcs at 0.367 nm. Occasionally, a reflection at 0.25 nm could be observed at an interplanar angle of 90° with respect to the 0.367 nm reflection (Fig. 4b). When the arcs were relatively wide, about 45°, it was difficult to determine the angles between the reciprocal lattice vectors accurately. However, from patterns with smaller arcs, it appeared that these angles were 68° ± 1° between the 0.414 nm reflections and 56° ± 1° between the 0.414 nm and 0.367 nm reflections.

An additional observation was that in the ED patterns of the CER and CER/CHOL samples, the intensity of one pair of the 0.41 nm reflections was occasionally stronger compared to the other two pairs of reflections (Fig. 2b). In the CER/CHOL/FFA samples, this difference in intensity between the two pairs with spacings at 0.41 nm has been found as well (Fig. 4b).

Diffraction patterns of the lipid mixtures were also recorded at tilt angles ranging from 10° to 30°. Under these conditions, some pairs of reflections disappeared so that ED patterns no longer consisted of rings or 6 opposite arcs, but consisted of opposite reflections scattered in one direction only (**Fig. 5**). The spacings of these reflections corresponded to those without tilting (about 0.41 nm and 0.37 nm).

DISCUSSION

The aim of this study was to investigate the lateral packing of lipids in dry lipid model systems using ED and to compare the results to WAXD data in literature from similar lipid mixtures. In contrast to WAXD, ED requires minimal amounts of lipid for the formation of detectable diffraction patterns. This implies that information can be obtained on the local structure and that within the area selected for diffraction relatively few orientations of the unit cells may be present.

A disadvantage of ED, however, can be the damaging effect of the primary electron beam on the sample. Therefore, in this study ED was not only performed at RT, but also under cryo-conditions to reduce radiation damage and the consequent fading of the diffraction patterns (31). The improved stability of the sample under cryo-conditions allowed us to increase the recording time by at least a factor 2. To avoid the interference of ice-crystal diffraction patterns with the diffraction patterns of lipids during cryo-ED, dry lipid samples were prepared. Based on results obtained from intact SC in which the lipid organization after dehydration was similar to that of hydrated SC (15, 16), it was hypothesized in the present study that the lack of wa-

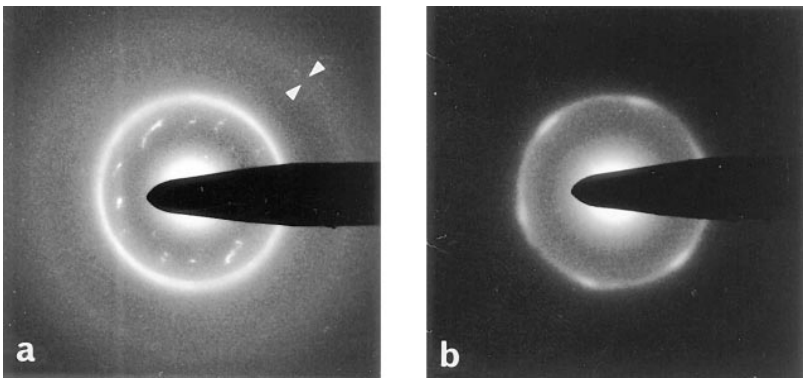

Fig. 3. Electron diffraction patterns of the CER/CHOL samples obtained from a: an area of 20 μm^2 and b: an area of 1 μm^2 in which the reflections are separated in arcs with an interplanar angle of 60° and an angular width of about 10°. In both patterns, reflections are present with spacings of 0.41 nm. Note in Fig. 3a the diffraction ring at 0.24 nm indicated by the arrowheads and the CHOL reflections.

Downloaded from www.jlr.org by guest, on June 14, 2012

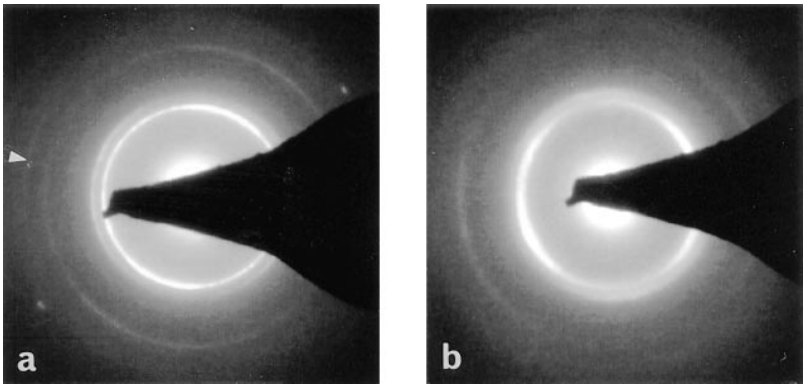

Fig. 4. Electron diffraction patterns of the CER/CHOL/FFA sample obtained from a: an area of 20 μm^2 and b: an area of 1 μm^2. In both patterns, the 0.41, 0.37, and 0.25 nm reflections are clearly visible. The arrowhead in Fig. 4a marks the reflection with a spacing of 0.22 nm. The interplanar angle between the 0.37 nm reflection and the 0.25 nm reflection in Fig. 4b is 90° and the angular width of the 0.41 nm reflections is about 45°. CHOL reflections are not always present.

ter in the lipid model system should not affect the lateral lipid organization. Of each sample, diffraction patterns were recorded at RT and at −170°C. The spacings measured at both temperatures did not differ significantly (see Table 1). From this, we conclude that the cooling procedure did not affect the lateral packing. Furthermore, the spacings that were calculated from the ED patterns of the CER/CHOL and CER/CHOL/FFA samples are in good agreement with WAXD data on dry lipid mixtures (unpublished results) and with WAXD results of wet lipid samples (8, 11). Therefore, we conclude that the spacings of the lateral lipid packing in our mixtures were not influenced by the absence of small amounts of water.

Interpretation of the electron diffraction patterns

We hypothesize that areas with different orientations of the lipid crystals can arise during the formation of the lipid layers on a grid. This may explain why certain areas gave rise to poor diffraction patterns or to only two opposite reflections, while other areas resulted in diffraction patterns with differently oriented pairs of reflections. When areas of these latter ED patterns were tilted >10°, some reflections disappeared while two opposite reflections mostly remained. Probably, areas that give rise to only two opposite reflections contain unit cells in a tilted position with respect to the incident electron beam, while areas that give rise to ED patterns with three pairs of arcs may have a more or less perpendicular orientation of the plane of the lipid layers. The finding that in some diffraction patterns the 0.41 nm reflections are not equally intense can also be explained by this tilting. From this we conclude that a proper orientation of the plane of the bilayers with respect to the incident electron beam is required to establish which lateral packing is present in the sample. Therefore, ED patterns from areas with a perpendicular orientation of the lipid layers were selected for interpretation.

The ED patterns of the CER samples are consistent with a hexagonal (non-crystalline) lattice, because one lattice spacing was found at 0.400 nm and the angles between the reciprocal lattice vectors were 60°. However, these results do not correspond to those obtained by Bouwstra et al. (8), who measured the spacings of the lateral lipid packing in CER mixtures using WAXD. In their study, they found reflections at 0.446, 0.435, 0.390, and 0.358 nm in these samples, which were attributed to a crystalline lipid packing not further defined. The discrepancy between these results may be explained by different preparation methods. The samples of Bouwstra et al. (8) underwent several freeze-thawing cycles to homogenize the CER mixture, while in the present study samples were prepared at RT. Indeed, Dahlen and Pascher (32) have shown that the crystalline structure of pure ceramides depends on the preparation method of the sample.

When we added cholesterol to the ceramides, the spacing calculated from the reflections in the diffraction patterns increased to 0.412 nm, other reflections were found at 0.24 nm, and the angles between the reciprocal lattice

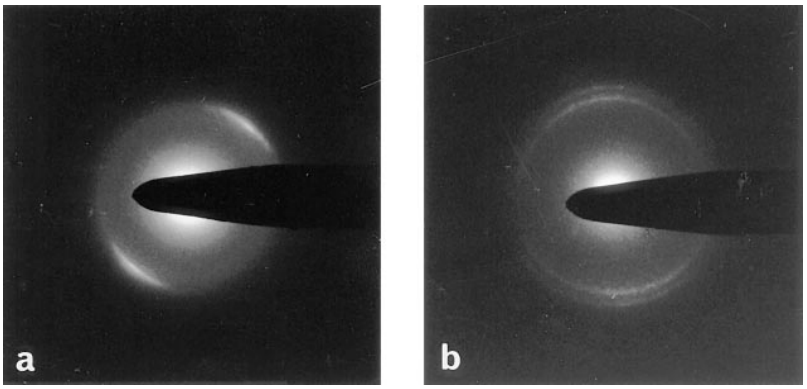

Fig. 5. Electron diffraction pattern of a: the CER/CHOL sample obtained at a tilt angle of 20° and b: the CER/CHOL/FFA sample obtained at a tilt angle of 10°. When the sample is tilted >10°, reflections already begin to disappear so that a unidirectionally scattered pattern remains.

Downloaded from www.jlr.org by guest, on June 14, 2012

vectors were 60°. These features are consistent with a hexagonal packing of the lipids. The hexagonal lattice and its corresponding diffraction pattern are shown schematically in **Fig. 6a**. Furthermore, in the CER/CHOL 1:1 mixture, reflections were found at smaller diffraction angles with spacings of 0.58, 0.52, 0.51, and 0.48 nm that correspond to those measured in the CHOL samples and with spacings known from literature (8, 15, 24). Therefore, we assign these reflections to crystalline anhydrous cholesterol. The observation that the cholesterol reflections appeared as spots regardless of the area selected for diffraction (1 μm^2 and 20 μm^2) indicates that the cholesterol crystals were not randomly oriented and that only a few (large) crystals were present. At higher CER/CHOL ratios or by addition of long-chain FFA, the cholesterol reflections disappeared largely, indicating that in these samples a smaller amount of cholesterol crystallized in a separate phase. This observation is in agreement with results obtained by SAXD (8).

The lattice spacing measured from the CER/CHOL mixtures (0.414 nm) was significantly larger ($P < 0.01$) than the lattice spacing in the pattern of the CER mixture, being 0.400 nm. The presence of cholesterol may be responsible for the alteration in the packing density. Abrahamsson et al. (33) investigated the influence of acyl chain length on the packing density and found that an increase in chain length resulted in an increase of the packing density. This was explained by the van der Waals forces, which become stronger with increasing chain lengths. The presence of the relatively short cholesterol molecules may, therefore, result in a decrease of those binding forces and, as a consequence, in a decreased packing density.

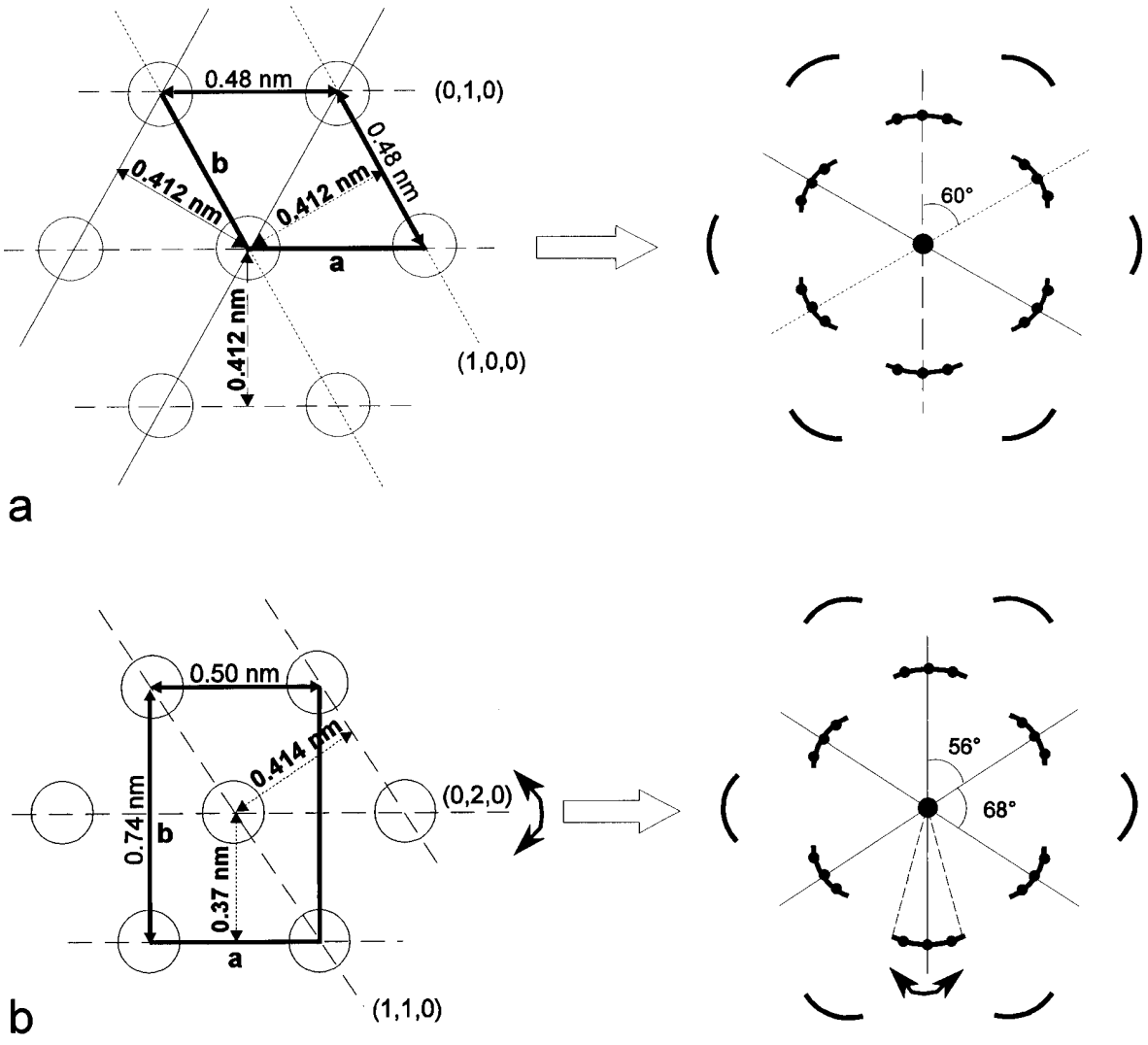

Fig. 6. Schematic drawing of the ordering of acyl chains and the corresponding diffraction patterns of a: the hexagonal lattice and b: the orthorhombic lattice (note the reciprocal relationship between the spacings in the lattice and the position of the reflections with respect to the central spot). This scheme outlines the molecular distances in the unit cells, the spacings between the lattice planes that produce the different reflections, the formation of arcs, and the angles between the reciprocal lattice vectors. The angular width of the arcs measured in degrees provides information on the extent to which the unit cells have rotated with respect to each other in the area selected for diffraction. This rotation of the unit cells may occur laterally or in depth.

Downloaded from www.jlr.org by guest, on June 14, 2012

The diffraction patterns of the CER/CHOL/FFA mixtures showed reflections at 0.414 and 0.367 nm, which is consistent with an orthorhombic lipid packing. Other features of this packing are the reflections at 0.25 and 0.22 nm and angles of 68° and 56° between the reciprocal lattice vectors. The orthorhombic lattice and the corresponding diffraction pattern are depicted in Fig. 6b. The finding that an orthorhombic lattice was formed in the presence of free fatty acids is in good agreement with the latest results of Bouwstra et al. (11). However, from their WAXD measurements, it could not be determined whether the hexagonal and orthorhombic packing were both present or only the orthorhombic packing. In our experiments, ED patterns were obtained from relatively small amounts of lipid compared to WAXD experiments. As a consequence, the number of unit cells and their orientations with respect to each other were also very small in the area selected for diffraction. Upon decreasing the irradiated area to 1 μm^2, diffraction patterns could consist of arcs instead of rings with an angular width of 15° to 25° in case of the CER and CER/CHOL samples and up to 45° in the CER/CHOL/FFA mixture. Due to this, additional information on the lipid packing was obtained by measuring the angles between the reciprocal lattice vectors in the ED patterns. On the basis of these angles and the position of the arcs, the presence of a hexagonal lattice in the CER/CHOL/FFA mixture can be excluded, because a third pair of reflections at 0.41 nm is absent (see Fig. 6 for comparison of the hexagonal and orthorhombic ED patterns). However, this does not mean that in the hydrated CER/CHOL/FFA samples prepared for WAXD measurements (11) no hexagonal phase was present either, because the influence of hydration on the SC lipids and their formation into a hexagonal or orthorhombic lattice is unknown.

The finding that in an area of approximately 1 μm^2 the reflections can be found separated in arcs indicates that within that region a certain orientation of the unit cells is maintained. The angular width of these arcs gives an indication of the degree of misalignment or the range of orientations of the unit cells in that area. Because our samples are multilayered, this rotation of the unit cells may not only occur laterally, but in depth as well. This suggests that one lipid layer may form a template for the next layer, so that a certain orientation is maintained. Apparently, the interaction between the lipid layers in the samples is so strong that lamellae can be formed comparable to those found in human SC. This has been shown by Bouwstra et al. (8) who studied similar models on mica sheets using SAXD. They found that models containing CER/CHOL/FFA are arranged in lamellae with both the long and short periodicities (12 and 6 nm).

In summary, the results of the present study clearly show the advantage of the application of ED for the recording of the lateral lipid organization in SC lipid models. We have shown by ED that the lipids in CER and CER/CHOL mixtures are arranged in a hexagonal packing, while in the CER/CHOL/FFA mixture the lipids are arranged in an orthorhombic lattice. The spacings measured in the samples are in very good agreement with those obtained by WAXD in similar models. Furthermore, we have demonstrated that ED is able to give very local information (areas of 1 μm^2) on the organization of SC lipids. In addition, it has been shown that ED allows the discrimination between the hexagonal and orthorhombic lipid packing on the basis of the 0.41 and 0.37 nm reflections, when the basal plane of the bilayers is oriented perpendicular to the incident electron beam. The fact that the ED and WAXD data correspond so well, means that ED can be used as an alternative and completely new method in skin studies. Using this technique in studies on intercellular domains of (human) SC, it will become possible to discriminate between regionally defined hexagonal and orthorhombic lattices.

The authors wish to thank L. D. C. Verschragen and H. M. van der Meulen for printing the micrographs and G. S. Gooris for providing the pig ceramides. Furthermore, we thank Prof. J. P. Abrahams for discussions. This research was supported by a grant (STW LGN44.3541) from the Dutch Society for Scientific Research (NWO).

Manuscript received 26 January 1998 and in revised form 23 April 1998.

REFERENCES

1. Matoltsy, A. G., A. M. Downes, and T. M. Sweeney. 1968. Studies of the epidermal water barrier. Part II. Investigations of the chemical nature of the water barrier. *J. Invest. Dermatol.* **50:** 19–26.
2. Elias, P. M. 1981. Lipids and the epidermal permeability barrier. *Arch. Dermatol. Res.* **270:** 95–117.
3. Nemanic, M. K., and P. M. Elias. 1980. In situ precipitation: A novel cytochemical technique for visualization of permeability pathways in mammalian stratum corneum. *J. Histochem. Cytochem.* **28:** 573–578.
4. Boddé, H. E., I. van den Brink, H. K. Koerten, and F. H. N. de Haan. 1991. Visualization of in vitro percutaneous penetration of mercuric chloride; transport through intercellular space versus cellular uptake through desmosomes. *J. Control. Release.* **15:** 227–236.
5. Elias, P. M., and D. S. Friend. 1975. The permeability barrier in mammalian epidermis. *J. Cell Biol.* **65:** 180–191.
6. Landmann, L. 1984. The epidermal permeability barrier. Comparison between in vivo and in vitro lipid structures. *Eur. J. Cell Biol.* **33:** 258–264.
7. Fenske, D. B., J. L. Thewalt, M. Bloom, and N. Kitson. 1994. Models of stratum corneum intercellular membranes: ^2H NMR of macroscopically oriented multilayers. *Biophys. J.* **67:** 1562–1573.
8. Bouwstra, J. A., G. S. Gooris, K. Cheng, A. Weerheim, W. Bras, and M. Ponec. 1996. Phase behavior of isolated skin lipids. *J. Lipid Res.* **37:** 999–1011.
9. McIntosh, T. J., M. E. Stewart, and D. T. Downing. 1996. X-ray diffraction analysis of isolated skin lipids: reconstitution of intercellular lipid domains. *Biochemistry.* **35:** 3649–3653.
10. Ten Grotenhuis, E., R. A. Demel, M. Ponec, D. R. Boer, J. C. van Miltenburg, and J. A. Bouwstra. 1996. Phase behavior of stratum corneum lipids in mixed Langmuir-Blodgett monolayers. *Biophys. J.* **71:** 1389–1399.
11. Bouwstra, J. A., G. S. Gooris, F. E. R. Dubbelaar, A. M. Weerheim, and M. Ponec. 1998. pH, cholesterol sulfate and fatty acids affect the stratum corneum lipid organization. *J. Invest. Dermatol.* In press.
12. Yamamura, T., T. Tezuka. 1989. The water-holding capacity of the stratum corneum measured by ^1H-NMR. *J. Invest. Dermatol.* **93:** 160–164.
13. Hou, S. Y. E., A. K. Mitra, S. H. White, G. K. Menon, R. Ghadially, and P. M. Elias. 1991. Membrane structures in normal and essential fatty acid-deficient stratum corneum: characterization by ru-

Downloaded from www.jlr.org by guest, on June 14, 2012

thenium tetroxide staining and X-ray diffraction. *J Invest. Dermatol.* **96:** 215–223.
14. Mak, V. H. W., R. O. Potts, and R. H. Guy. 1991. Does hydration affect intercellular lipid organization in the stratum corneum. *Pharm. Res.* **8:** 1064–1065.
15. Bouwstra, J. A., G. S. Gooris, M. A. Salomons-de Vries, J. A. van der Spek, and W. Bras. 1992. Structure of human stratum corneum as a function of temperature and hydration: a wide-angle X-ray diffraction study. *Int. J. Pharm.* **84:** 205–216.
16. Gay, C. L., R. H. Guy, G. M. Golden, V. H. W. Mak, and M. L. Francoeur. 1994. Characterization of low-temperature (i.e., $< 65°C$) lipid transitions in human stratum corneum. *J. Invest. Dermatol.* **103:** 233–239.
17. Boddé, H. E., H. L. G. M. Tiemessen, H. Mollee, F. H. N. de Haan, and H. E. Junginger. 1990. Modelling percutaneous drug transport in vitro: The interplay between water, flux enhancers and skin lipids. *In* Predictions of Percutaneous Penetration: Methods, Measurements, Modelling. 5th ed. R. C. Scott, R. H. Guy, and J. Hadgraft, editors. 1BC Technical Services.
18. Alonso, A., N. C. Meirelles, V. E. Yushmanov, and M. Tabak. 1996. Water increases the fluidity of intercellular membranes of stratum corneum: Correlation with water permeability, elastic, and electrical resistance properties. *J. Invest. Dermatol.* **106:** 1058–1063.
19. Wertz, P. W., and D. T. Downing. 1991. Epidermal lipids. *In* Physiology, Biochemistry, and Molecular Biology of the Skin. Volume I. L. A. Goldsmith, editor. Oxford University Press, Oxford. 205–236.
20. Craane-van Hinsberg, I. W. H. M., J. C. Verhoef, F. Spies, J. A. Bouwstra, G. S. Gooris, H. E. Junginger, and H. E. Boddé. 1997. Electroperturbation of the human skin barrier in vitro: II. Effects on stratum corneum lipid ordering and ultrastructure. *Microsc. Res. Tech.* **37:** 200–213.
21. Madison, K. C., D. C. Swartzendruber, P. W. Wertz, and D. T. Downing. 1987. Presence of intact intercellular lipid lamellae in the upper layers of the stratum corneum. *J. Invest. Dermatol.* **88:** 714–718.
22. Van der Meulen, J., B. A. I. van den Bergh, A. A. Mulder, A. M. Mommaas, J. A. Bouwstra, and H. K. Koerten. 1996. The use of vibratome sections for the ruthenium tetroxide protocol: a key for optimal visualization of epidermal lipid bilayers of the entire human stratum corneum in transmission electron microscopy. *J. Microsc.* 184: 67–70.
23. Bouwstra, J. A., G. S. Gooris, J. A. van der Spek, and W. Bras. 1991. Structural investigations of human stratum corneum by small-angle scattering. *J. Invest. Dermatol.* **97:** 1005–1013.
24. Bouwstra, J. A., G. S. Gooris, W. Bras, and D. T. Downing. 1995. Lipid organization in pig stratum corneum. *J. Lipid Res.* **36:** 685–695.
25. Chen, Y. L., and T. S. Wiedmann. 1996. Human stratum corneum lipids have a distorted orthorhombic packing at the surface of cohesive failure. *J. Invest. Dermatol.* **107:** 15–19.
26. Harrison, J. E., P. W. Groundwater, K. R. Brain, and J. Hadgraft. 1996. Azone® induced fluidity in human stratum corneum. A Fourier transform infrared spectroscopy investigation using the perdeuterated analogue. *J. Control. Release.* **41:** 283–290.
27. Garson, J. C., J. Doucet, J. L. Lévêque, and G. Tsoucaris. 1991. Oriented structure in human stratum corneum revealed by X-ray diffraction. *J. Invest. Dermatol.* **96:** 43–49.
28. White, S. H., D. Mirejovsky, and G. I. King. 1988. Structure of lamellar lipid domains and corneocyte envelopes of murine stratum corneum. An X-ray diffraction study. *Biochemistry.* **27:** 3725–3732.
29. Wijdeveld, M. M. G., H. K. Koerten, J. J. M. Onderwater, D. T. Parrott, and J. A. Bouwstra. 1996. Visualization and electron diffraction on cryosections of stratum corneum: a utopia? *J. Microsc.* **183:** 223–230.
30. Pilgram, G. S. K., A. M. van Pelt, F. Spies, J. A. Bouwstra, and H. K. Koerten. 1998. Cryo-electron diffraction as a tool to study local variations in the lipid organization of human stratum corneum. *J. Microsc.* **189:** 71–78.
31. Ohno, T. 1996. Fading and broadening of electron diffraction spot from beam-damaged multiple monolayer films. *J. Microsc.* **184:** 17–21.
32. Dahlen, B., and I. Pascher. 1979. Molecular arrangements in sphingolipids. Thermotropic phase behaviour of tetracosanoylphytosphingosine. *Chem. Phys. Lipids.* **24:** 119–133.
33. Abrahamsson, S., B. Dahlen, H. Lofgren, and I. Pascher. 1978. Lateral packing of hydrocarbon chains. *Prog. Chem. Fats Other Lipids* **16:** 125–143.

Downloaded from www.jlr.org by guest, on June 14, 2012